A Concept of a Hybrid WDM/TDM Topology Using the Fabry-Perot Laser in the Optiwave Simulation Environment

Radek POBORIL[1], Jan LATAL[1], Petr KOUDELKA[1], Jan VITASEK[1], Petr SISKA[1], Jan SKAPA[1], Vladimir VASINEK[1]

[1]Department of Telecommunications, Faculty of Electrical Engineering and Computer Science, VSB – Technical University of Ostrava, 17. listopadu 15, 708 33 Ostrava, Czech Republic

radek.poboril@gmail.com, jan.latal@vsb.cz, petr.koudelka@vsb.cz, jan.vitasek@vsb.cz, petr.siska@vsb.cz, jan.skapa@vsb.cz, vladimir.vasinek@vsb.cz

Abstract. *The aim of this article is to point out the possibility of solving problems related to a concept of a flexible hybrid optical access network. The entire topology design was realized using the OPTIWAVE development environment, in which particular test measurements were carried out as well. Therefore, in the following chapters, we will subsequently focus on individual parts of the proposed topology and will give reasons for their functions whilst the last part of the article consists of values measured in the topology and their overall evaluation.*

Keywords

Hybrid PON network, WDM, TDM, WDM/TDM, Fabry-Perot laser, AWG, topology design, Optiwave.

1.   Introduction

The motivation of passive optical network (PON) technology is to provide a cost-effective access mechanism to end-users, which is interference-free and bandwidth-abundant. The general PON topology consists of single mode fibres linking the optical line terminal (OLT) and the optical network units (ONUs) with an optical distribution network (ODN). Based on this, TDM-PON technology is already mature [1].

Since the end users begin to use Internet services such as HDTV, VOIP, gaming or video conference, their demands for the bandwidth will exceed 100 Mb·s^{-1} by the end of 2012. In 2009 in Japan, the number of users connected via optical fibre exceeded 17 million. Copper lines and wireless access methods are not able to meet these requirements and that is why the attention is turning to the use of optical fibres [2], [3].

Passive optical networks got their name because of the fact that they don't use powered devices in the outside infrastructures, i.e. don't use so called active amplifiers or splitters and hubs, elements providing splitting of the light output power into branches. Passive splitters are used instead of active elements and allow dividing signal among many users. Typically, the optical signal is divided among 16, 32, 64 or 128 users within the maximum distance of 10-20 km. The passive network's big advantage over the active one is the fact it can be expanded relatively cheaply.

Time-division multiplexing and wavelength-division multiplexing belong among the most popular multiplex methods. The time-division multiplex method is used especially for short distances within metropolitan networks etc. while the wavelength-division multiplex one is used for long distances, such as for example backbone networks.

Each of these multiplex methods has its pros and cons. Time-division multiplex is able to serve only a small number of participants – with low speed, however, for reasonable prices. On the other hand, wavelength-division multiplex can serve a high number of participants but its price is much higher.

In light of these different properties, there is an effort to create a hybrid network that would have positive characteristics of both of these multiplexes and at the same time would meet the characteristics of the passive optical network [4], [5].

The Stanford University ACCESS (SUCCESS) initiative within the Photonics & Networking Research Laboratory encompasses multiple projects in access networks. One of these projects is the Hybrid TDM/WDM PON or SUCCESS-HPON [6], [7].

2. Hybrid PON

Time division multiplexing (TDM) and wavelength-division multiplexing (WDM) technologies have their pros and cons and therefore, in order to obtain the best topology properties for signal transmission, combinations of these two multiplex methods are being developed. The disadvantages of TDM are the advantages of WDM. The time-division multiplex is not able to fully exploit the optical fibre possibilities, and the wavelength-division multiplex is quite expensive as for the implementation. Their unification brings about good transmission properties for favorable economic aspect of the project. As for remote operation between OLT and ONT, we use the WDM multiplex. It is then divided by the arrayed waveguide gratings (AWG) demultiplexer into individual wavelengths, which are then sent to the topology. A part of the network, which is behind the WDM demultiplexer, already uses the TDM multiplex. That is why the TDM demultiplexer is located as close as possible to the target area, which is served by the access network [8], [9].
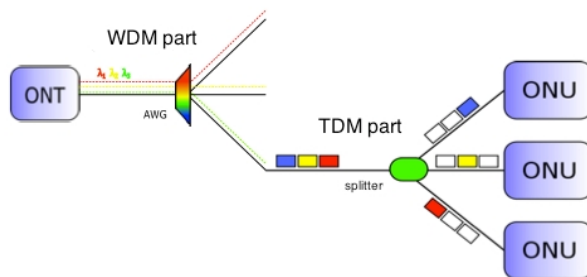

Fig. 1: Hybrid passive optical network.

3. A Topology Design in the Environment Optiwave

As for the transfer, our topology uses the L band and C band. The L band is used for downstream and the C band for upstream. Thanks to using dense wavelength-division multiplexing (DWDM) technology, we used 32 wavelengths with 100 GHz spacing in each band. The each channel's speed is 10 Gbit·s^{-1}, the topology total transfer rate is thus 320 Gbit·s^{-1} bidirectionally on a single fibre (full duplex). Every wavelength is then multiplexed using TDM for two ONUs.

The entire concept can be divided into several sections: transmitters, receivers, fabry perot (FP) laser feed, outside plant and elements before and behind the plant. In the following chapters, we will have a look at the setting and implementation of the individual parts [10], [11], [12], [13].

3.1. Transmitters

In the transmitting section, we chose the continuous wave laser with the output power 5,5 dBm. We used CW_laser_Array instead of several continuous wave lasers and it helped us to group all the 32 lasers together. The adjustment was relatively simple. Parameters were set to these values: initial frequency – 186 THz, spacing – 100 GHz, output power – 5,5 dBm, number of outputs – 32, noise – 100 dBm. For the sake of clarity, the output from CW_Laser_Array was then multiplexed into a single beam using the AWG with the inner attenuation of 3 dB. This option can be or doesn't have to be used in a real connection. It would depend on the level of integration of each component. The signal located at the multiplex output is shown in Fig. 2.
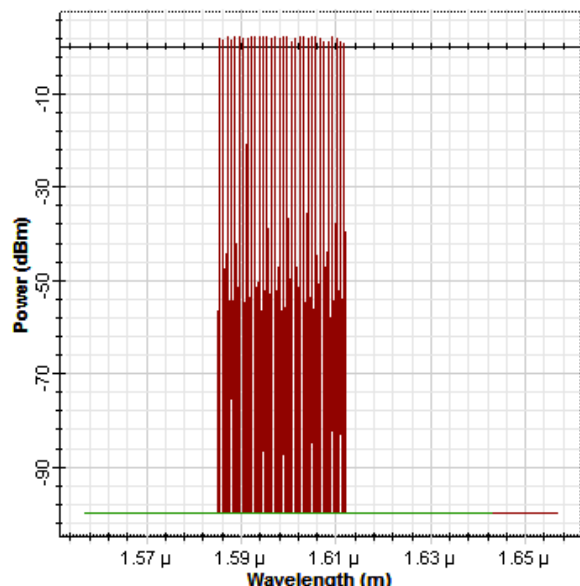

Fig. 2: Signal on multiplexer output.

Continuous wave laser is not an ideal source of radiance for the FP cavity. According to the Optiwave documentation, the FP cavity is used in conjunction with a white light source that passes through the Gaussian filter and then feeds the FP cavity. In our case, it would not be possible because a white light source can't be used in connection with the TDM multiplex. We also tried to use other lasers such as Pump Laser, however, this one didn't work with the TDM multiplex either.
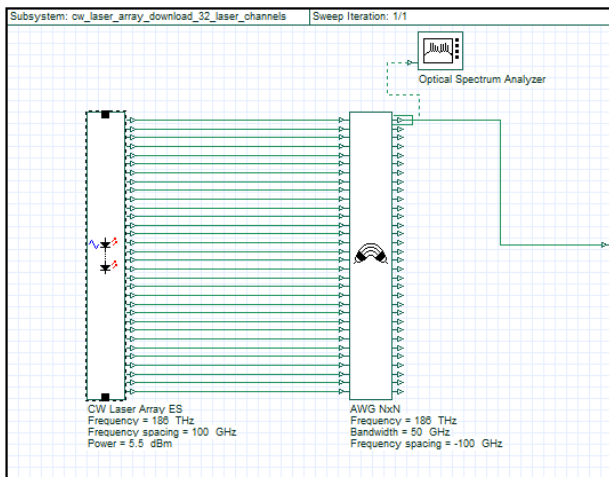
Fig. 3: Light source for Fabry-perot lasers.

The output light beam then goes to another sub-schema where it is divided into individual wavelengths and assigned through FP filters to FP cavities. As for the FP filters, we set the desired mean value of frequency (according to the wavelength we wanted to establish in the FP) and bandwidth which is sufficient for the proper function of amplitude modulation and which later doesn't affect the surroundings wavelengths. Experimental measurements enabled us to find out that an ideal method for feeding FP laser is to use the white light source in combination with the Gaussian filter. However, despite the fact that the signal appearing at the output laser was sufficient according to an optical spectrum analyzer (OSA), it was not sufficient for the proper function of the subsequent application of the time-division multiplex.

After the advent of the filtered beam, the FP laser binds to its wavelength, which is then amplified and radiated away. As for the simulation, this wavelength is at its output. Data signal is created using PRBS generator (Pseudorandom binary sequence generator) and is brought to a pulse generator input with a return-to-zero (RZ). In the next step, the signal is processed in a sub-schema called TDM transmitter.
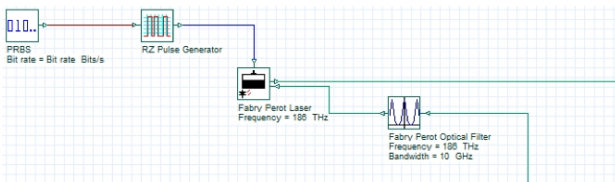

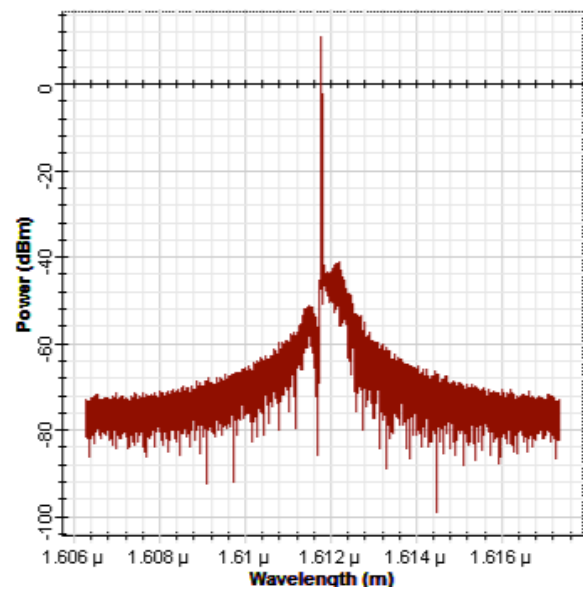**Fig. 4:** Circuit layout of Fabry-perot laser.

Fig. 5: Fabry-perot output signal.

Figure 6 shows the inner design of a part of the implemented connection that operates the optical time-division multiplexing (OTDM). After the signal is brought into the sub-schema, it is divided into N parts, where N is the number of channels created subsequently. After its division, the signal is brought into the Amplitude Modulation (AM) input. The signals are modulated using the same carrier frequency [13].

Again, PRBS and RZ generators are control elements. It is also necessary to use a time delay before the modulated signals are merged into one using a power combiner. As far as the first channel is concerned, its delay is zero and the element is inserted for the sake of transparency. As for the second channel, its delay is defined according to the following formula:

$$Delay[s] = \frac{1}{B} \cdot \frac{A}{N}, \tag{1}$$

where B is a bit rate, A is an order of channels (counted from zero) and N is a number of channels [13].
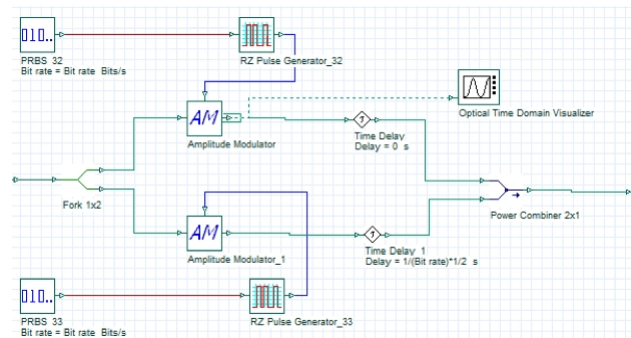

Fig. 6: Implementation of TDM multiplex.

After TDM multiplexing is completed, the signal is ready for transmission. This sequential filtering, amplification and TDM multiplexing is done for all 32 channels. Using the AWG, all these channels are then merged into a single beam, which is connected with the multiplexer before the path.

Figure 7 shows the output signal from a part of the TDM transmitter. There is a power level of randomly generated pulses. Thanks to this random generating the graph shows 2 types of signal power level. From zero to 6,5 mW approximately and from 6,5 mW to 13 mW approximately. Each TDM transmitter channel has its own PRBS and thus there can be a situation when generators generate a pulse at the same time. These pulses then have a higher power level than other pulses because their power is summed up.
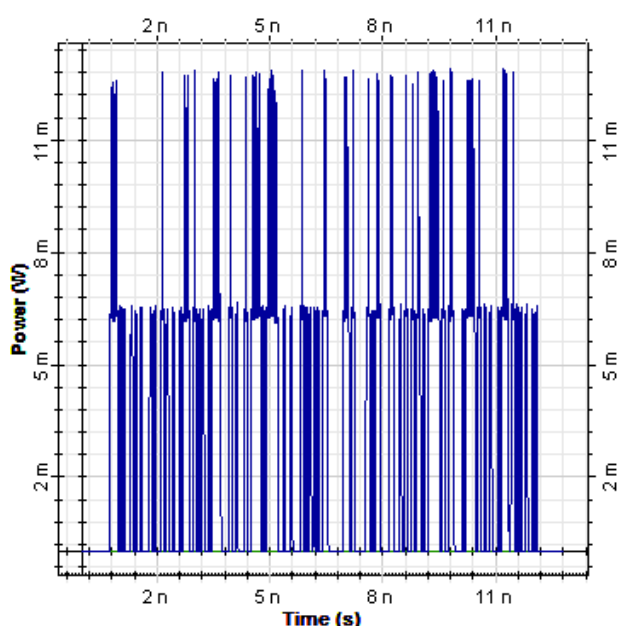

Fig. 7: Two channels in Time-division multiplex.

3.2. Feeding FP Laser

FP lasers were used mainly because of their possibility to tune themselves to the incoming wavelength and because of their possible spectral width for WDM. Thanks to this feature, it is not necessary that continuous wave lasers are on the side of ONU. The continuous wave lasers are located at the side of OLT. Thanks to this, the provider is allowed to manipulate the used wavelengths more easily. Therefore, we created a sub-schema called „cw_laser_array_upstream_feed_32_channels", which contains a continuous wave laser field, the AWG multiplexer and the EDFA amplifier [13].

We set the first frequency for the laser field to 191 THz and the subsequent spacing for the 32 channels to 100 GHz. The output power was set to 5,5 dBm. Outputs from the laser field were then multiplexed into a single

beam and amplified. EDFA amplifier has a gain control setting. That is why we set the gain value to 5 dB. Of course, we also had to set the noise occurring in active elements. In our case, we used 3 dB. The central value of the noise frequency was set to 192,5 THz and the noise bandwidth to 5 THz. Noise was then in the whole spectrum of 32 channels.
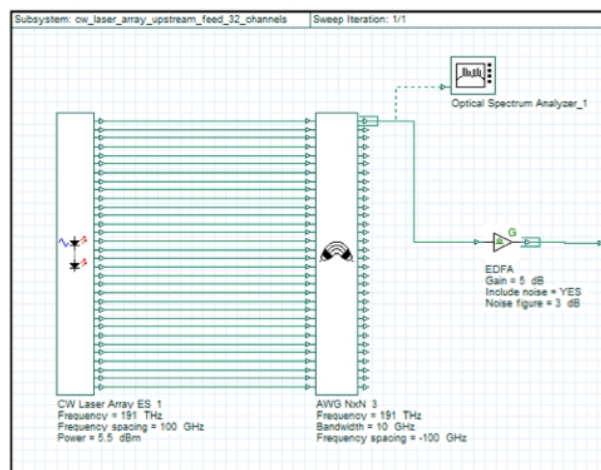

Fig. 8: Lasers for FP feeding.

From the economic point of view, it is much more expedient to multiplex the outputs from the continuous wave laser into a single beam first and then to amplify, than to amplify each channel separately first and then to multiplex.
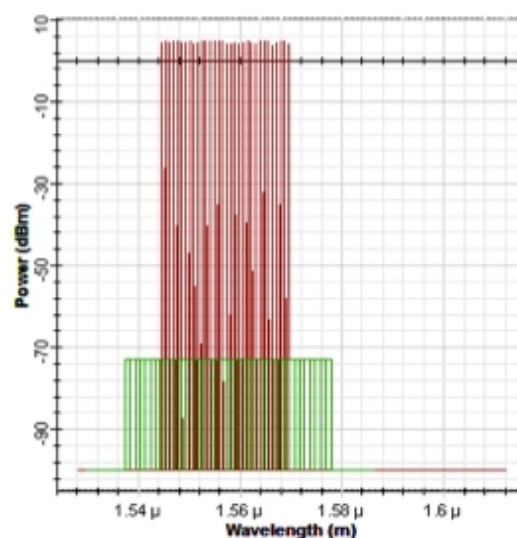

Fig. 9: The spectral characteristics at the output of EDFA amplifiers.

3.3. Transmission Medium

As far as a simulation of the transmission medium is concerned, we chose on optical fibre with preset parameters from the Optiwave library. Since the aim of our concept was to transmit upstream and downstream

over a single fibre, we had to choose a bidirectional version of this fibre. Length of the tested path was 2, 5 and 10 km at full-duplex speed 320 Gbit·s^{-1} on 32 channels, i.e. 10 Gbit·s^{-1} per channel. Basic parameters of the fibre corresponded to G.652.C/D fibre and we present them in the table below.

Tab.1: Features of G.652 C/D fibre.

Parameter	Value	Unit
Fibre length	2; 5; 10	km
Attenuation	0,25	dB·km^{-1}
Dispersion	16,75	ps·nm^{-1}·km
Start dispersion	0,075	ps·nm^{-1}·km
Temperature	300/27	K/°C
Rayleigh scattering	50·10^{-6}	km^{-1}
Dynamic noise	3	dB

In the simulation program, it is necessary for the right functionality of the bidirectional fibre to add optical delay into reverse direction. We put the optical delay before and behind the optical fibre, see Fig. 8. We set every delay to 1. Another important parameter was a number of iterations of the simulation program. This can be set in Layout Parameters/Signal Iterations X, where X is the total number of all optical delays in the path of a signal +1. In our case, the X was 3 (X=3).
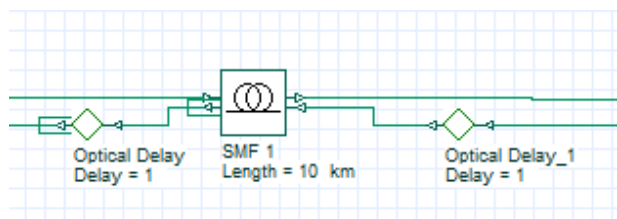

Fig. 10: Bidirectional fibre.

The optical delay is very important in a simulation because without it we would be able to calculate only one direction in bidirectional components. This is connected with the subsequent displaying on imaging elements where we must set the signal index. If we talk about the signal before the optical delay, the index is 0. If the signal is after the delay, the index equals the number of iterations -1.

3.4. Elements Before and Behind the Outside Plant

Since we used the FP lasers that need a feeding signal, the fibre has to transmit two beams of signals in a single direction. The first one is the downstream signal and the second one is the feeding for FP lasers on the side of ONU. That is why we merged these two signals into a single one using a multiplexer. We used a two-channel multiplexer where a value of the first channel was set to 187,5 THz and the second one to 192,5 THz. We needed the multiplexer to merge two beams comprising of

several channels into two channels only and hence we had to adjust the width of the first as well as of the second channel of the multiplexer to 5 THz. In this case, an ideal filter for this was a rectangular one [13].
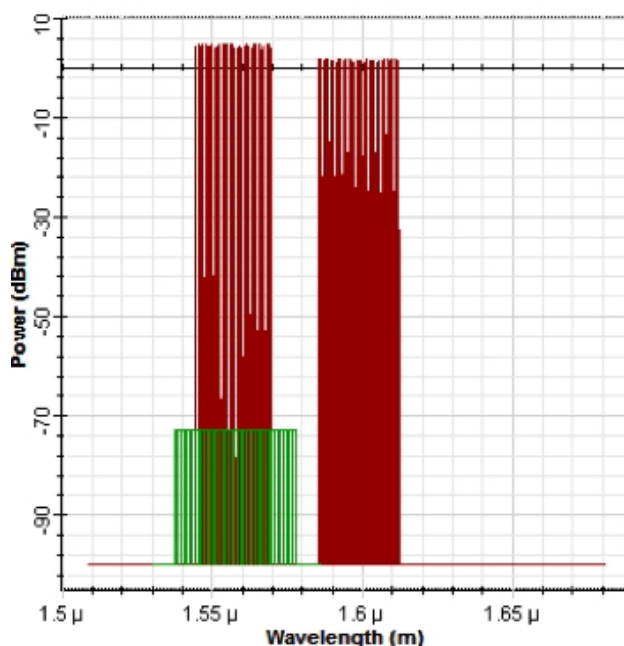
Fig. 11: Spectral characteristic on multiplexer output before line.

3.5. Receivers

The last important parts of the concept are the receivers. These are implemented in the sub-schema "Receivers". Using the AWG demultiplexer, a signal arriving at its input is divided into individual wavelengths. In order to maintain the right functionality of the NxN AWG, all the unconnected inputs must be connected to the optical zero. And to do this, there is an optical "nuller". The particular channels are then divided into two through the use of a power splitter. As for the first signal, no delay is applied to it, while as for the second one, there is a delay according to the formula (1). Both signals are then modified in the same way. An avalanche photodiode (APD) is set to capture the signal with the highest level. The APD dark current is 10 nA. The ASE noise is turned on as well in order to reach the most realistic connection.
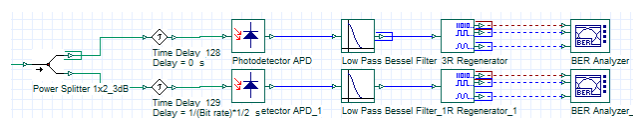
Fig. 12: Layout of receivers.

Low-pass filter is another important element. Its boundary frequency is set to 8 GHz. The filter removes the high frequency noise resulting from the signal passing through its path due to nonlinearities, dispersion etc. Since the high frequency noise does not meet the Shannon-Kotelnik theorem requirements, there is an

effect called aliasing. This effect is undesirable and that is why it is removed with the help of low pass filter which can also be called anti-aliasing filter.

The sampling theorem is given by the formula:

$$f_{VZ} = 2 \cdot f_N \geq 2 \cdot f_{MAX} [Hz], \qquad (2)$$

where f_{max} is the maximum frequency contained in the signal sampling, and f_n is the Nyquist frequency, thus the highest frequency which can be sampled properly at the given sampling frequency.

Figure 13 and Fig. 14 show connections without a low pass Bessel filter and with it, respectively. A 3R regenerator restores the shape and the time base of the signal and amplifies it. The last element, a bit error rate (BER) analyzer, tells us the exact properties of the signal after its passing through the entire topology. And we will analyse these properties in the subsequent chapter.
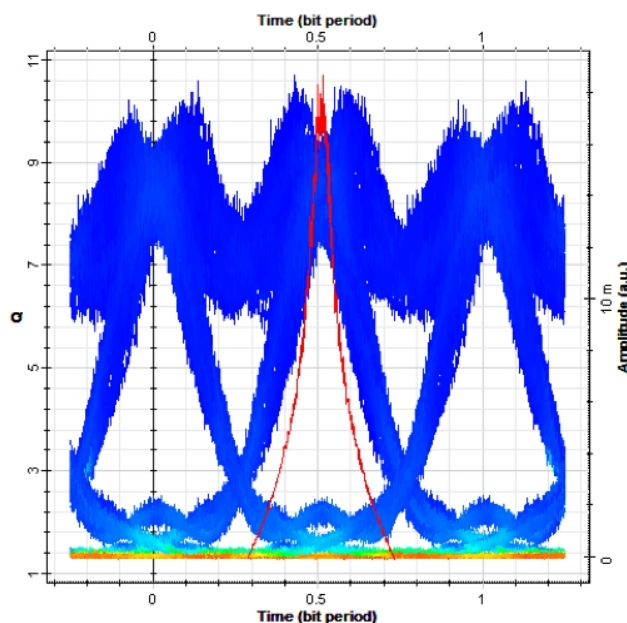

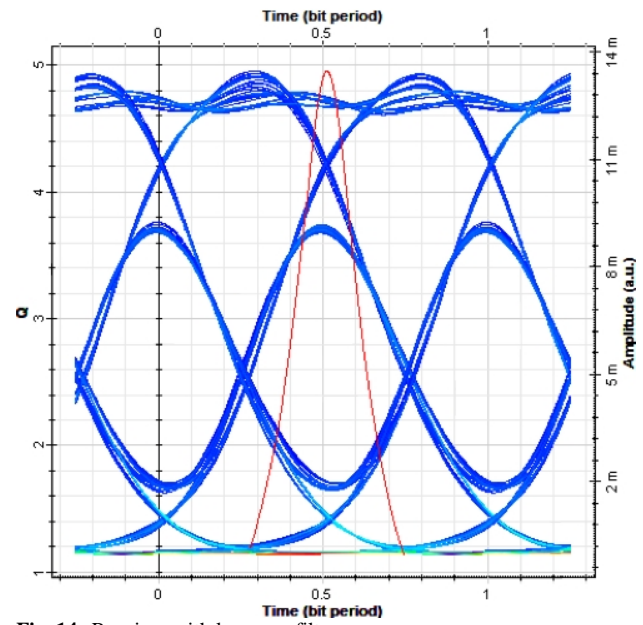**Fig. 13:** Receiver without low pass filter.

Fig. 14: Receiver with low pass filter.

4. The Topology Evaluation

In this chapter, we are dealing with the precisely measured properties of the topology. Parameters tested are the following: the total path attenuation, the drop of the output power between the transmitter and the receiver, and the quality of the signal whose basic properties are the Q factor, the bit error rate and the eye diagram.

The topology will be tested in downstream and upstream, with the path length 2, 5 and 10 km, and with the speed $10 \text{ Gbit} \cdot \text{s}^{-1}$ and 1 Gbit per channel. In the following chapters we will test the first channel of the downstream and the upstream.

4.1. Attenuation

The total path attenuation is the sum of all the attenuations on the path from the transmitting laser to the receiver. We set the attenuation to 3 dB for all the elements on the path, the attenuation on the path itself is 0,25 dB/km. As for the upstream, we have to allow for the fact that the signal will pass through the line 2 times owing to the location of the FP laser feeding on the side of OLT, therefore we inserted the EDFA amplifier with a 5 dB gain behind the feeding lasers. The results are shown in the following tables:

Tab.2: Downstream attenuation.

Line length [km]	2	5	10
Attenuation[dB]	25,28	26	27,2

Tab.3: Upstream attenuation.

Line length [km]	2	5	10
Attenuation[dB]	26,76	28,2	30,6

Considering the topology structure, the measured attenuation values are all right. The attenuation was gradually increased together with the length of the tested path. As for the upstream, we could detect an increased attenuation due to the effect of the Fabry-Perot lasers, which need a light source feeding. With such a large number of participants, a difference between AWG and an ordinary splitter is very visible. AWG has an advantage over splitter because the attenuation does not increase with a number of its outputs, as it is in the case of splitter. Thank to this feature, the designed topology is much more flexible for the option of a possible increase of participants.

4.2. Drop of the Output Power Level

The drop of the output power level gives us the output power loss level between two measured points in the topology. For our topology, we chose these locations.

For the downstream:

- point A is located behind the multiplexer for feeding lasers of the downstream,

- point B is located behind the demultiplexer splitting the signal of the downstream and feeding the signal for the upstream.

For the upstream:

- point C is located behind the EDFA amplifier of the feeding signal,

- point D is located at the end of the transmission path for the upstream.

Tab.4: Drop of output power on line 2 km.

Bit rate [Gbit·s⁻¹]	10	1
Drop of output level [dBm] downstream	8,231	6,423
Drop of output level [dBm] upstream	7,387	5,579

Tab.5: Drop of output power on line 5 km.

Bit rate [Gbit·s⁻¹]	10	1
Drop of output level [dBm] downstream	8,944	7,143
Drop of output level [dBm] upstream	8,207	6,408

Tab.6: Drop of output power on line 10 km.

Bit rate [Gbit·s⁻¹]	10	1
Drop of output level [dBm] downstream	10,144	8,334
Drop of output level [dBm] upstream	9,566	7,766

4.3. Bit Error Rate (BER)

1) Q Factor

Q factor or quality factor gives us the quality of signal with respect to distance of signal from the noise. It covers all the noises, dispersions and nonlinearities, which deteriorate the signal quality and thereby increase the bit error rate. It follows that the higher Q factor, the higher signal quality. Q factor is defined according to the following formula:

$$Q = \frac{v_1 - v_0}{\sigma_1 - \sigma_0}[-], \qquad (3)$$

where v_1 is a logic level "1", v_0 is a logic level "0", σ_1 is a standard deviation of a logic level "1" and σ_0 is a standard deviation of a logic level "0".

As for the first channel of our topology, we measured out the following Q factor:

Tab.7: Line length 2 km.

Bit rate [Gbit·s⁻¹]	10	1
Q-factor [-] downstream	6,24143	6,70096
Q-factor [-] upstream	6,29794	6,60824

Tab.8: Line length 5 km.

Bit rate [Gbit·s⁻¹]	10	1
Q-factor [-] downstream	5,99217	6,66647
Q-factor [-] upstream	6,04626	6,67962

Tab.9: Line length 10 km.

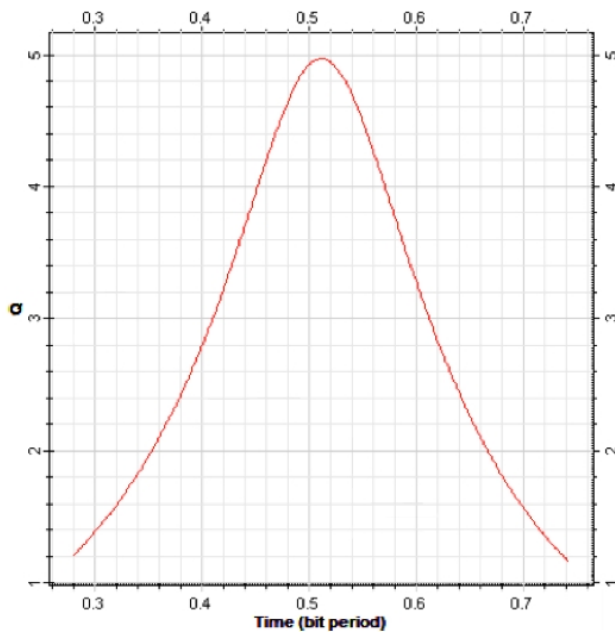| Bit rate [Gbit·s⁻¹]	10	1
Q-factor [-] downstream	4,97226	6,66709
Q-factor [-] upstream	5,39022	6,69558

Fig. 15: Q-factor on 10 km line with bit rate 10 Gbit·s^{-1}.

The Q-factor value is closely dependent on the BER value. If the Q-factor value is 6, the BER value is 10^{-9}. The values measured in our topology confirm this relation. When decreasing the Q-factor value, the bit error rate was increasing [16].

2) Bit Error Rate

Bit error rate is one of the main indicators of the quality of optical connection. It is under the influence of the same parameters as the Q factor. Bit error rate gives us the ratio between the number of mistakenly received bE bits and the total number of the received p bits in dependence on time. The relationship is given by the formula:

$$BER = \frac{bE}{v \cdot t}[-], \qquad (4)$$

where v is bit rate and t is time of measurement.

As for the first channel of our topology, we measured out the following BER:

Tab.10: Bit error rate on line 2 km.

Bit rate [Gbit·s^{-1}]	10	1
BER [-] downstream	1,97167·10^{-10}	9,68781·10^{-12}
BER[-] upstream	1,36624·10^{-10}	1,81217·10^{-11}

Tab.11: Bit error rate on line 5 km.

Bit rate [Gbit·s^{-1}]	10	1
BER [-] downstream	9,37714·10^{-10}	1,21384·10^{-11}
BER[-] upstream	6,71759·10^{-10}	1,11986·10^{-11}

Tab.12: Bit error rate on line 10 km.

Bit rate [Gbit·s^{-1}]	10	1
BER [-] downstream	3,0043·10^{-7}	1,2178·10^{-11}
BER[-] upstream	320037·10^{-8}	1,05422·10^{-11}

The BER parameter values measured in our topology were found in the range from 10^{-7} to 10^{-12}, as expected. Professional literature specifies this value as the maximum and minimum BER value respectively necessary for the correct transmission over the topology. The BER parameter value was changing in dependence on the bit rate and the length of the tested route [16].

3) Eye Diagram

The eye diagram shows the superposition of all mutually overlapping bits in the signal. The **eye opening** indicates the differentiability of the logic 1 from the logic 0. The more the eye is wide open, the greater the differentiability is, because it's better signal noise to ratio. Other eye-readable parameters are: **jitter** (delay fluctuation), intersymbol interference (**ISI**) and time length of **rising or falling edge** [14] [16].
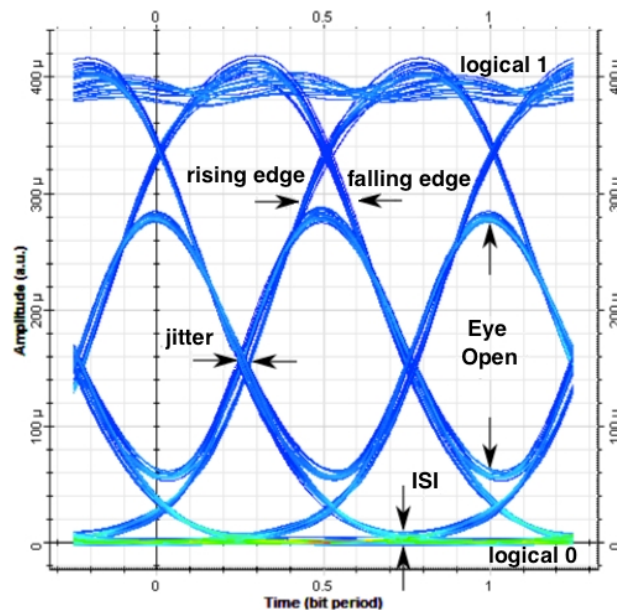

Fig. 16: Eye diagram description.

The following figures show the eye diagrams of the first channel at speeds 10 Gbit·s^{-1} on the path length 2, 5 and 10 km downstream.
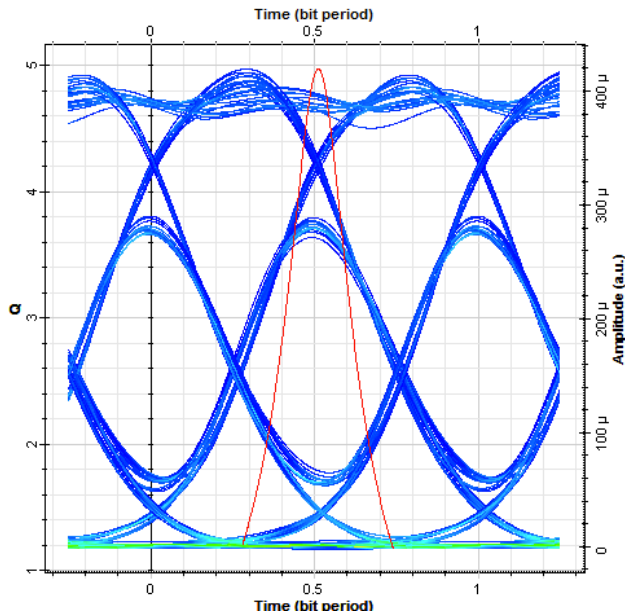
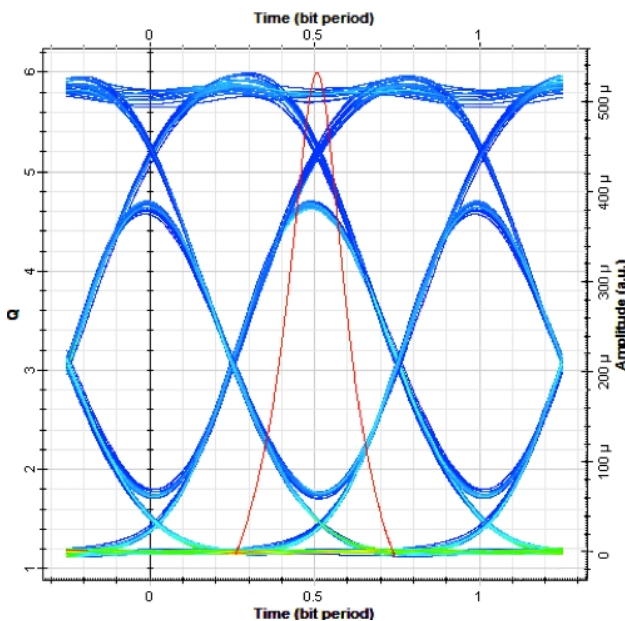**Fig. 17:** Eye diagram showing the first channel of the topology with 10 Gbit·s⁻¹ on fiber length 10 km.
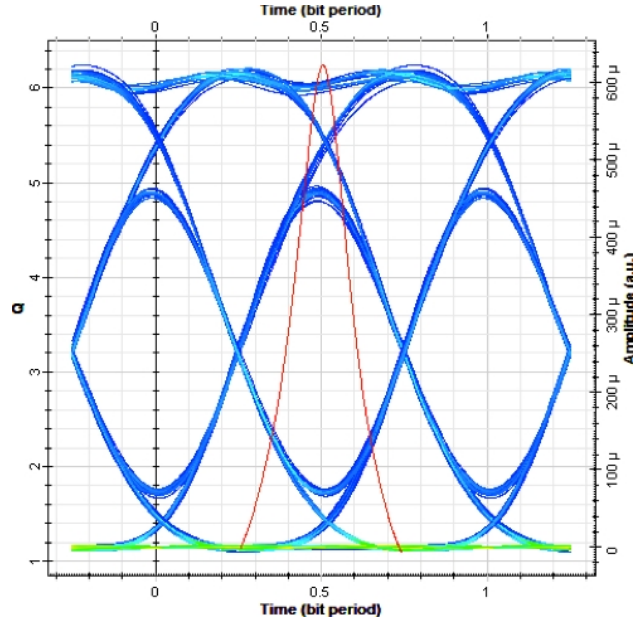

Fig. 19: Eye diagram showing the first channel of the topology with 10 Gbit·s⁻¹ on fiber length 2 km.

Parameters of the particular eye diagrams correspond with the measured values, which we have already mentioned in the previous parts of this chapter. It is clearly seen that the Q-factor is lower when the route length is 10 km than when it is 2 km. On the other hand, jitter is increased due to the effect of dispersion. Nevertheless, the measured parameters are still normal and a signal transmission would be realizable.

4.4. Comparison of APD and PIN Diode Properties

Another experiment was to compare the quality of signal receiving as for the APD and PIN diode. The experiment confirmed our theoretical assumptions, namely that, thanks to its greater sensitivity, the APD diode has better BER as well as Q factor values. Therefore, we used the APD diodes for our concept. The following figures show the individual outputs from the BER analyzer of the APD and PIN photodetector. The measuring was performed at a transmission speed 10 Gbit·s⁻¹ on the 10 km long path. Setting the photodetectors was very similar. Responsivity of both diodes was set to 1 A·W⁻¹ and the dark current value was 10 nA. However, as for the APD diode, there was a possibility to set up two more parameters - the gain to the value 3 and the ionization ration to the value 0,9 [15].
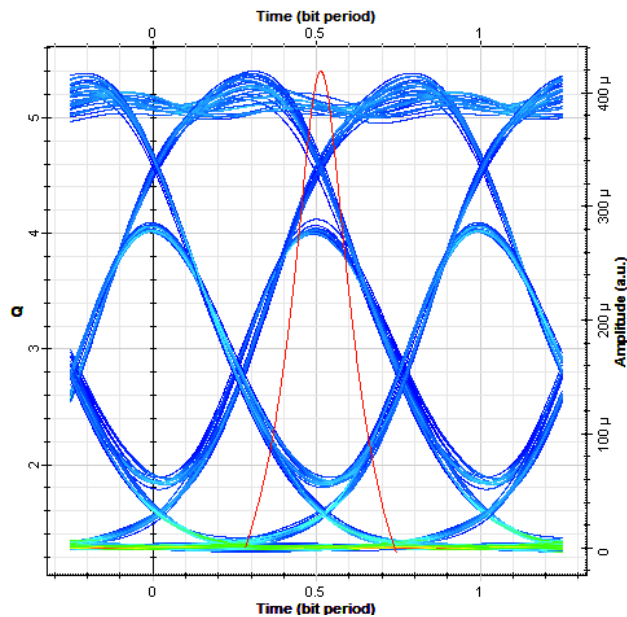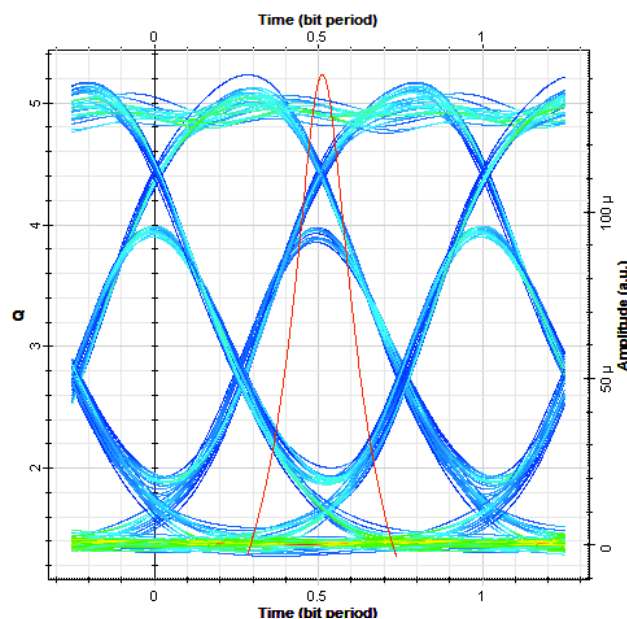

Fig. 18: Eye diagram showing the first channel of the topology with 10 Gbit·s⁻¹ on fiber length 5 km.

Fig. 20: Eye diagram of APD diode.

Fig. 21: Eye diagram of PIN diode.

Tab.13: APD diode eye analysis.

Max. Q Factor [-]	5,40191
Min. BER [-]	$3{,}08541 \cdot 10^{-8}$
Eye Height [-]	$1{,}39913 \cdot 10^{-4}$
Total Power [dBm]	-42,892
Noise Power [dBm]	-82,795

Tab.14: PIN diode eye analysis.

Max. Q Factor [-]	5,2307
Min. BER [-]	$7{,}92033 \cdot 10^{-8}$
Eye Height [-]	$4{,}46535 \cdot 10^{-5}$
Total Power [dBm]	-52,434
Noise Power [dBm]	-86,879

5. Conclusion

Hybrid access networks are a very important solution that will be used profusely in the future, thanks to its key properties such as large data transfer rate for a large number of participants for favourably low prices. This article describes one of an immense number of ways how to design a network. We used tree architecture and modern components in dependence on wavelength such as FP lasers and AWG routers. All the simulations had the expected results. The bit rate of 320 Gbit·s^{-1} for 32 channels duplex is sufficient for the 10 km distance. At this transmission rate, the bit error rate ranged from 10^{-7} to 10^{-12}, which are satisfactory results. It follows that a hybrid WDM/TDM PON is a quality future proof solution offering a great potential. In the next article, we will focus on different types of coding, light sources, modulations, on their influence on transmission quality for the given topology and on a test concerning the maximum possible number of participants.

Acknowledgements

References

[1] LIN, R. Next generation PON in emerging networks. In: *OFC/NFOEC 2008 - 2008 Conference on Optical Fibre Communication/National Fibre Optic Engineers Conference*, art. no. 4528701. IEEE, 2008. pp. 1-3, ISBN 978-1-55752-856-8.

[2] KIMURA, S. WDM/TDM-PON Technologies for Future Flexible Optical Access Networks, In: *OptoeElectronics and Communications Conference (OECC)*, IEEE, 2010. pp. 14 – 15, ISBN 978-1-4244-6785-3.

[3] QIU, S.; HUANG, J.; GUO, X.; LUO, J, T.; ZHANG, Z, Z. A novel hybrid WDM/TDM optical passive network architecture. In *Proceedings of SPIE - The International Society for Optical Engineering* 6354 II, art. no. 63543K. IEEE, 2006. ISBN 978-081946449-1. doi:10.1117/12.691062.

[4] AHSAN, Shamim; LEE, Seop, Man. Migration to the Next Generation Optical Access Networks Using Hybrid WDM/TDM-PON, *Journal of Networks*, 2011, Vol. 6, No. 1, pp. 18-25. ISSN 1796-2056.

[5] LEE, S.; KIM, E.; LEE, Y.; LEE, S.; JUNG, D.; HWANG, S.; OH, Y.; PARK, J. A design of WDM/TDM-PON provisioning for future optical access network upgrade. *IEICE TRANSACTIONS on Communications*, 2007. Vol. E90-B, No. 9, pp. 2456-2463. ISSN 1745-1345.

[6] AN, F.-T.; GUTIERREZ, D.; KIM, K., S.; LEE, J., W.; KAZOVSKY, L., G. SUCCESS-HPON: A next-generation optical access architecture for smooth migration from TDM-PON to WDM-PON. 2005. *IEEE Communications Magazine*, Vol. 43, No. 11, pp. S40 - S47. ISSN 0163-6804.

[7] GUTIERREZ, D.; KIM, K., S.; AN, F.-T.; KAZOVSKY, L., G. SUCCESS-HPON: Migrating from TDM-PON to WDM-PON. 2006. In: *European Conference on Optical Communications Proceedings, ECOC 2006* , art. no. 4801079. 2006. pp. 1-2, ISBN 978-2-912328-39-7.

[8] ABRAMS, M.; BECKER, P., C.; FUJIMOTO, Y.; O'BYRNE, V.; PIEHLER, D. FTTP Deployments in the United States and Japan: equipment choices and service provider imperatives, *Journal of Lightwave Technology*, 2005. Vol. 23, No. 1, pp. 236-246. ISSN 0733-8724.

[9] DAVEY R., KANI J., BOURGART F., MCCAMMON K. Options for future optical access networks. *IEEE Communications Magazine*, 2000, Vol. 44, No. 10, pp. 50-56. ISSN 0163-6804.

[10] HLADKÝ, Miroslav; ŠIŠKA, Petr. *WDM PON je DWDM-PON : EXPERIMENTÁLNÍ PRACOVIŠTE WDM PON na VŠB v Ostravě* [online]: 2011 [cit. 2011-04-25]. Available at WWW: <http://www.profibre.eu/files/A8_Hladky_Siska_WDM-PON_je_DWDM-PON.pdf>.

[11] ŠÍMA, Jaromír. *RLC Praha a.s.* [online]. 2005 [cit. 2011-04-26]. *DWDM pro metropolitní síte*. Available at WWW: <http://www.rlc.cz/publikujeme/dwdm_metro/>.

[12] CHENG, Ning; EFFENBERGER, Frank. WDM PON: Systems and Technologies. In *European Conference and Exhibition on Optical Communication* [online]. 2010, Available at WWW: <http://www.ecoc2010.org/contents/attached/c20/WS_5_Cheng.pdf>.

[13] Optiwave [online]. [cit. 2011-04-26]. Available at WWW: <http://optiwave.com/>.

[14] TEJKAL, Vladimír. et al. Dvoustavové modulační formáty v optických přístupových sítích. *Advances in Electrical and Electronic Engineering*. 2010, Vol. 8, No. 4. pp. 96-101. ISSN 1804-3119.

[15] MIROSLAV, Filka. *Optoelektronika pro telekomunikace a informatiku*. Brno: Centa, spol. s r.o., 2009. pp. 371. ISBN 978-80-86785-14-1.

[16] KAZOVSKY, Leonid G., et al. *Broadband Optical Access Networks*. Canada: Wiley, 2011. pp. 283. ISBN 978-0-470-18235-2.

About Authors

Radek POBORIL was born in Valasske Mezirici. He received his B.Sc. Degree from the Technical University of Ostrava, Faculty of Electrical Engineering and Computer Science in 2011. Currently in Master degree studies, he focuses on optical technologies and especially on WDM/TDM PON.

Jan LATAL was born in Prostejov. He received his B.Sc. Degree from the VSB-Technical University of Ostrava, Faculty of Electrical Engineering and Computer Science, Dept. of Electronic and Telecommunications in 2006. He received his M.Sc. Degree from the Technical University of Ostrava, Faculty of Electrical Engineering and Computer Science, Dept. of Telecommunications in 2008. Currently in doctor degree studies, he focuses on optical technologies (xPON) and especially on free space optics, fibre optics sensors etc. He is member of SPIE.

Petr KOUDELKA was born in 1984 in Prostejov. In 2006, he finished bachelor study at VSB-Technical University of Ostrava, Faculty of Electrical Engineering and Computer Science, Dept. of Electronic and Telecommunications. Two years later, he finished M.Sc. in the field of optoelectronics. In the present time during his Ph.D. study he is interested in Free Space Optics and Distributed Temperature Sensing systems.

Jan VITASEK was born in 1984 in Opava. In 2009 he finished M.Sc. study at Brno University of Technology, Faculty of Electrical Engineering and Communication. In present time he is Ph.D. student at VSB – Technical University of Ostrava. His interests are propagation and processing of optic signals.
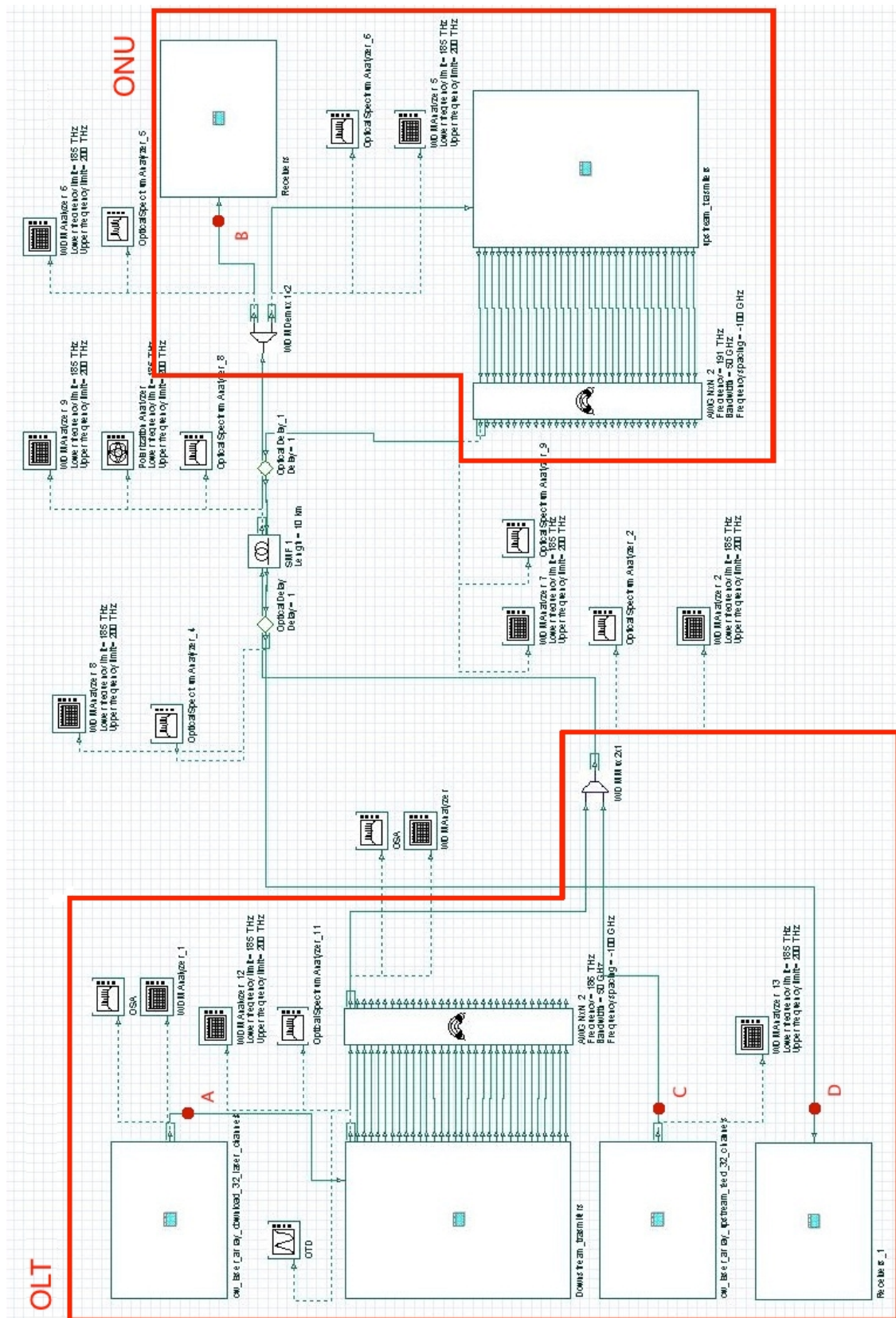
Petr SISKA was born in 1979 in Kromeriz. In 2005 he finished M.Sc. study at VSB-Technical University of Ostrava, Faculty of Electrical Engineering and Computer Science, Dept. of Electronic and Telecommunications. Three years later, he finished Ph.D. study in Telecommunication technologies. Currently he is employee of Department of Telecommunications. He is interested in Optical communications, Fibre optic sensors and Distributed Temperature Sensing systems.

Jan SKAPA was born in Ostrava, Czech Republic in the year of 1980. He reached the Ph.D. in Telecommunication technologies in 2009. He's professional interests involves optical communication systems, optical fibre sensors, digital signal processing and speech and image processing.

Vladimir VASINEK was born in Ostrava. In 1980 - he graduated at the Science Faculty of the Palacky University, branch - Physics with specialization in Optoelectronics, RNDr. he obtained at the Science Faculty of the Palacky University at branch Applied Electronics, scientific degree Ph.D. he obtained in the year 1989 at branch Quantum Electronics and Optics, he became an associate professor in 1994 at branch Applied Physics, he is a professor of Electronics and Communication Science since 2007 and he works at this branch at the Department of Telecommunications of the Faculty of Electrical Engineering and Computer Science. His research work is dedicated to optical communications, optical fibres, optoelectronics, optical measurements, optical networks projecting, fibre optic sensors, MW access networks. He is a member of many societies - OSA, SPIE, EOS, Czech Photonics Society, he is a chairman of Ph.D. board at the Technical University of Ostrava, and he was a member of many boards for habilitation and professor appointment.

Appendix A. Hybrid WDM/TDM topology.

Appendix A. Hybrid WDM/TDM topology.